ICANS-XIII
13th Meeting of the International Collaboration on
Advanced Neutron Sources
October 11-14, 1995
Paul Scherrer Institut, 5232 Villigen PSI, Switzerland

THE MCLIB LIBRARY: MONTE CARLO SIMULATION OF NEUTRON SCATTERING INSTRUMENTS

Philip A. Seeger

239 Loma del Escolar, Los Alamos, NM 87544, USA
E-mail: PASeeger@aol.com

ABSTRACT

This report describes the philosophy and structure of MCLIB, a Fortran library of Monte Carlo subroutines which has been developed to test designs of neutron scattering instruments. A pair of programs (LQDGEOM and MC_RUN) which use the library are shown as an example.

1. Introduction

Monte Carlo is a method to integrate over a large number of variables. Random numbers are used to select a value for each variable, and the integrand is evaluated. The process is repeated a large number of times and the resulting values are averaged. For a neutron transport problem, we first select a neutron from the source distribution, and project it through the instrument using either deterministic or probabilistic algorithms to describe its interaction whenever it hits something, and then (if it hits the detector) tally it in a histogram representing where and when it was detected. This is intended to simulate the process of running an actual experiment (but it is *much* slower). Monte Carlo is a useful supplement to analytical treatment of an instrument, in particular to check and demonstrate "non-intuitive" focusing arrangements.

The present MCLIB library has been derived from codes written by Mike Johnson at the Rutherford Laboratory [1]. Significant additions and revisions were made by this author in 1984 [2], and the entire code was rewritten in a structured form in 1994 [3]. Whenever the code has been applied to new problems, additions have been made. Thus significant contributions to the present library have been made by Richard Heenan (Rutherford-Appleton Laboratory), and by Glenn Olah, Bob VonDreele, Greg Smith, and Luke Daemen (Los Alamos neutron Science Center, LANSCE). Mike Fitzsimmons and Joyce Goldstone have contributed greatly to the debugging process. Several applications of the code were presented at an instrument design workshop [4]. A new collaboration with Larry Passell and Uli Wildgruber (Brookhaven National Laboratory) is also producing improvements.

The process is carried out in two stages. First a program must be generated to describe the geometry of the specific instrument being simulated; for example, the program LQDGEOM may be used to define a small-angle scattering instrument with pinhole collimation, up to three

Keywords: MCLIB, Monte Carlo, simulation, instruments

choppers, and an on-axis 2-dimensional position sensitive detector. Essentially all of the user interaction occurs in this stage. The output is a geometry file containing the complete problem definition. That file is then passed to a second-stage program, for example MC_RUN, which transports neutrons and tallies results in histograms. Principal outputs are a file with a statistical summary, and a data file with histograms of the spectrum and detector. A third stage, which is not part of the Monte Carlo process, is to perform whatever data reduction is appropriate to the experiment being simulated. Some measure of the information content (or a "figure of merit") is then used to evaluate the design of the instrument.

Features of MCLIB which are different from other Monte Carlo libraries include

- Simplified transmission through materials. Rather than compute microscopic interaction in a simple (amorphous unpolarized) region, attenuation of the transmitted neutron is calculated.
- Optics at surfaces. When a neutron reaches a surface, the (complex) index of refraction is computed to decide whether the neutron will reflect or refract.
- Time-dependent devices. There are element types to describe moving devices such as choppers or a gravity focuser.
- Acceleration of gravity is included in transport.
- Scattering functions. Each kind of scattering sample is an element type. The scattering algorithm may be deterministic (reflectometry), probabilistic (hard-sphere scatterer), or a combination (Bragg reflection into a Debye-Scherrer cone).

2. Geometry Description by Surfaces and Regions

The geometry of a system is described by surfaces and regions. A *surface* is defined by a general 3-dimensional quadratic equation of the form

$$A\,x^2 + B\,x + C\,y^2 + D\,y + E\,z^2 + F\,z + G + P\,xy + Q\,yz + R\,zx = 0 \qquad (1)$$

with 10 coefficients, plus a roughness parameter (*BETA*). The surface divides 3-dimensional space into two parts, which are called the + and – sides of the surface depending on whether the left-hand side of eq. (1) evaluates to a positive or a negative value. For example, a plane perpendicular to the z-axis at z = 1 can be expressed by the equation

$$z - 1 = 0,$$

i.e., $F = 1$ and $G = -1$ (all other coefficients zero). Then all points with $z < 1$ are on the – side and all points with $z > 1$ are on the + side of the surface. The scaling of eq. (1) is arbitrary, but we tend to evaluate it as m^2, so that coefficients A, C, E, P, Q, and R are dimensionless, coefficients B, D, and F are in m, and G is m^2. The parameter *BETA* is the length of a randomly oriented 3-dimensional vector which is added to the unit vector normal to the mathematical surface to determine the surface orientation when a particle interacts. For a perfect smooth surface, $BETA = 0$; for $0 < BETA < 1$, *BETA* is the sine of the maximum angular deviation of the surface normal from smooth. If $BETA < 0$ (or $BETA >> 1$), the surface is completely random.

Note that the coordinate system being used is left handed: the instrument axis is the positive z-direction, the x-axis is horizontal and positive to the right, and the y-axis is vertical with the acceleration of gravity in the negative y-direction.

The geometric shape of each *region* is defined by its relationship to all of the defined surfaces. A positive or negative integer is placed in the region definition if every point in the region is on the + or – side of the corresponding surface, and surfaces which do not bound the region are set to zero. Special characteristics of the boundary are given by the value of the integer: ±1 for an ordinary surface with roughness *BETA* and the possibility of refraction or critical reflection; ±2 for total reflection; ±3 for diffuse scattering (independent of *BETA*); ±4 for total absorption; and ±5 for cases requiring special action (such as a coordinate transformation) whenever a particle enters or leaves the region. Generally, no surface may be used as a boundary of a region if any part of that surface is inside the region, because then some points in the region would be on the + side and some on the – side of that surface. Concave (reentrant) shapes are allowed when using quadratic surfaces as in fig. 1a, but the shape in fig. 1b requires that two regions be defined. Another method to define a reentrant region is to exclude embedded regions, which is accomplished by adding 10 to the surface type number in the definition of the enclosing region (*e.g.*, "4" becomes "14" or "–1" becomes "–11"). Such surfaces are *not* tested as part of the definition of being inside the region. When the trajectory of a particle inside the region intersects the surface, it will exit if a valid region exists on the other side, but will otherwise remain in the enclosing region. This method must be used with care, since particles within the embedded regions also pass the test for being within the enclosing region.

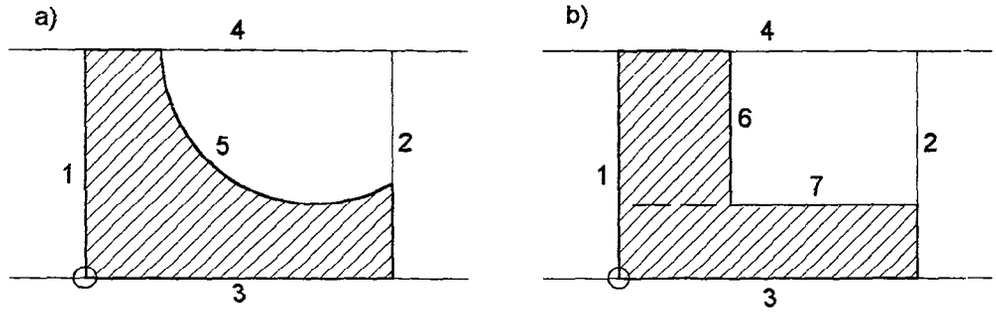

Figure 1. Concave regions.

Equations of the numbered surfaces are

1:		x				=	0		
2:		x			– 4	=	0		
3:				y		=	0		
4:				y	– 3	=	0		
5:	x^2	– 6 x	+ y^2	– 6 y	+ 14	=	0	or	$(x-3)^2 + (y-3)^2 = r^2 = 4$
6:		x			– 1.5	=	0		
7:				y	– 1	=	0		

The shaded area in a) can be expressed unequivocally as a single region:

+1 −1 +1 −1 +1 0 0

To avoid ambiguity, the area in b) requires two regions, divided as shown by surface 7 (or alternatively by surface 6).

+1 −1 +1 0 0 0 −1
+1 0 0 −1 0 −1 +1

The unshaded area in either case requires 5 regions for a complete unambiguous definition. (One choice of region boundaries is shown by the faint lines.) If the upper right corner

0 −1 0 −1 0 +1 +1

is considered an embedded region, then the shaded area may also be defined as

+1 −1 +1 −1 0 −11 −11

3. Instrument Elements

Each region is also an *element* of the instrument. Every element has a *NAME* and a pointer (*INDEX*). For a void drift region, *INDEX* = 0, and for every element which is not a void

INDEX points to a location in a REAL*4 parameter block which contains the element type number, possibly followed by additional parameters. Future development of the library should be accomplished by defining new element types and implementing the corresponding algorithms for how a neutron interacts in such regions. Presently defined types and their parameters are listed below; file MC_ELMNT.INC (Appendix A) includes definitions of mnemonic symbols for all the parameters, with values equal to the address offset from the *INDEX* pointer.

type 0 = total absorber; no parameters
type 1 = amorphous unpolarized material; 4 parameters
Real and Imaginary scattering-length density (10^{10}/cm^2)
macroscopic scattering cross section (1/m)
velocity-dependent cross section, at 1 m/μs (1/μs)
type 2 = aluminum, including Bragg edges; no parameters
type 3 = hydrogenous, including multiple scattering
type 4 = supermirror represented by trapezoidal reflectivity; 4 parameters
Real & Imaginary scattering-length density (10^{10}/cm^2) (see type 1)
Supermirror multiplier
Reflectivity at maximum supermirror limit
type 5 = beryllium at 100K, including Bragg edges; no parameters
type 6 = single-crystal filter, Freund formalism; 3 parameters
$\Sigma = \Sigma_{free} \times \{1 - \exp(-C_2/\lambda^2)\} + \Sigma_{abs} \times \lambda$
Σ_{free} = limiting (short wavelength) free-atom macroscopic cross section (1/cm)
$C_2 = -\ln\{1 - (\Sigma(1Å) - \Sigma_{abs})/(\Sigma_{free} - \Sigma_{abs})\}$ (Å^2)
Σ_{abs} = sum of 1/v macroscopic cross sections at 1Å (1/cm/Å)
type 10 = multi-aperture collimator
type 11 = multi-slit collimator, vertical blades; 3 or 5 parameters
Note: the type 11 region must be followed immediately by up to 5 additional regions defining the center passage and the bounding blades, and the entrance/exit surfaces must be surface type 5.
Spacing of slits, centerline-to-centerline (m)
Rate of convergence (>0) or divergence (<0) of one slit
Z at entrance of the region, where spacing is measured (m)
For a curved system (bender),
sine of half the angle of bend
cosine of half the angle of bend
type 12 = multi-slit collimator, horizontal blades; 3 or 5 parameters
Same parameters as type 11 (see *Note* under type 11)
type 13 = crystal monochrometer; 10 parameters
Twice the crystal plane spacing (Å)
Nominal Z position for rotation of instrument axis (m)
Sine and cosine of take-off angle
X-, Y-, and Z-components of mosaic spread, rms of sines of angles
rms spread of plane spacing, σ_d/d
max number of loops (or microcrystal orientations) to try
probability normalization factor per try, derived from reflection probability at peak wavelength: $1 - (1 - \text{max\_prob})^{(1/\text{trys})}$
types 20.n = chopper (disk or blade); 6 parameters
20.0 or 20.2 for motion in x-direction, 20.1 or 20.3 for y-direction

20.2 or 20.3 is counter-rotating (fully closed when edges at 0)
Linear velocity of opening crossing beam centerline (m/μs)
Time to cover or uncover half the width of the moderator (μs)
Nominal time at which opening chopper edge crosses zero (μs)
Nominal time at which closing chopper edge crosses zero (μs)
Phase jitter of chopper, rms (μs)
Period of chopper (μs)

type 21 = Fermi chopper (not implemented)

type 22 = gravity focuser; 5 parameters
Note: the type 22 region must be followed immediately by 2 additional regions defining the aperture, and the entrance/exit surfaces must be surface type 5.
acceleration (m/μs^2), and rms phase jitter (μs)
nominal times for start and top of upward stroke (μs)
time between pulses (μs)

type 23 = removable beamstop; no parameters

type 30 = sample which scatters at constant Q; 2 parameters
–ln(transmission at 1 Å)
value of Q for scatter (1/Å)

type 31 = scattering sample of hard spheres; 2 parameters
–ln(transmission at 1 Å)
hard-sphere radius for scatter (Å)

type 32 = isotropic scatterer with fixed energy change; 2 parameters
–ln(transmission at 1 Å)
inelastic energy change (0 if elastic) (meV)

type 34 = inelastic scattering kernel; no parameters; *NAME* is '[path]filename' of $S(\alpha,\beta)$ file in MCNP Type I format

type 35 = scattering from layered reflectometry sample; 1 + 4 *N* parameters
number of layers, including substrate
parameters for each layer, starting with substrate:
4π x Real and Imaginary scattering-length density (1/Å^2)
Thickness of layer (zero for substrate) (Å)
Roughness, 2 σ^2 of outer surface of this layer (Å^2)

type 36 = scattering from isotropic polycrystalline powder; 6 parameters + 2 × table length
number of Bragg edges included
limiting (short wavelength) macroscopic total xsection (1/cm)
macroscopic incoherent scattering cross section (1/cm)
macroscopic 1/v scattering cross section at 1 Å (1/cm/Å)
macroscopic 1/v absorption cross section at 1 Å (1/cm/Å)
table of d-spacings of Bragg edges (Å), followed by explicit 0 and table of cumulative macroscopic cross sections at 1 Å (1/cm/Å^2)

type 40 = detector; 9 parameters
surface number
–ln(1 – efficiency at 1 Å)
time-of-flight clock parameters:
minimum and maximum times (μs)
number of time channels
if logarithmic, dt/t (otherwise dt/t = 0)
minimum clock tick in determining log scale (μs)

electronic delay of detector events (μs)
repeat period of data-acquisition electronics (μs)
Note: if t-o-f is logarithmic, *TMAX* is overridden

type 41 = vertical linear detector; 14 parameters
surface number
–ln(1 – efficiency at 1 Å)
time-of-flight parameters (7)
locations of bottom and top of detector (m)
number of detector elements
size of detector element (m)
root-mean-square encoding error of detector (m)

type 42 = horizontal linear detector; 14 parameters
surface number
–ln(1 – efficiency at 1 Å)
time-of-flight parameters (7)
locations of left and right ends of detector (m)
number of detector elements
size of detector element (m)
root-mean-square encoding error of detector (m)

type 43 = 2-D rectilinear detector; 18 parameters
surface number
–ln(1 – efficiency at 1 Å)
time-of-flight parameters (7)
locations of left and right edges of detector (m)
number of detector elements in the horizontal direction
width of detector element (m)
root-mean-square X encoding error of detector (m)
locations of bottom and top edges of detector (m)
number of detector elements in the vertical direction
height of detector element (m)
root-mean-square Y encoding error of detector (m)

type 44 = longitudinal linear detector; 14 parameters
surface number
–ln(1 – efficiency at 1 Å)
time-of-flight parameters (7)
locations of upstream and downstream ends of detector (m)
number of detector elements
size of detector element (m)
root-mean-square encoding error of detector (m)

type 50 = scattering chamber, void-filled. No parameters, but other regions may be embedded, indicated by surface types with 10s digit on.

types 90.n = source size and phase space to be sampled; 14-18 parameters
edges of rectangular moderator face (m)
location and radius (half-width) of apertures which define beam (m)
additional vertical space to sample for gravity focus (m)
min and max neutron energy to be sampled (eV)
time between beam pulses and square pulse width (μs)
offset to parameter block with spectrum and line shape parameters
(optional) half-heights of apertures, type 90.1 or 90.2 (m)

(optional) vertical offsets of apertures, type 90.4 (m)

type 91 = source energy distribution table and line shape parameters; 12 parameters plus length of table
number of entries in energy table (1 is special case)
location in table of center of normal distribution (index units)
or value of nominal neutron velocity (m/μs) (if number of entries = 1)
standard deviation of normal distribution (table index units)
or relative fwhm of velocity selector (if number of entries = 1)
source brightness, summed over limits of *E_TABLE* (n/ster/m^2/MW/s)
1 or 2 exponential time constants in thermal (low-energy) limit (μs)
probability of 2nd exponential
epithermal (high energy) time constant proportional to λ (μs/Å)
or mean (t/λ) parameter of Ikeda-Carpenter form (μs/Å) (if width < 0)
Gaussian delay and width proportional to λ (μs/Å) (width<0 is special case)
switching function 1/e point (Å) and power (slope)
origin of table of cumulative energy distribution (weighted by λ^2) of source spectrum on equally spaced normal-curve values of log(E / 1 meV)

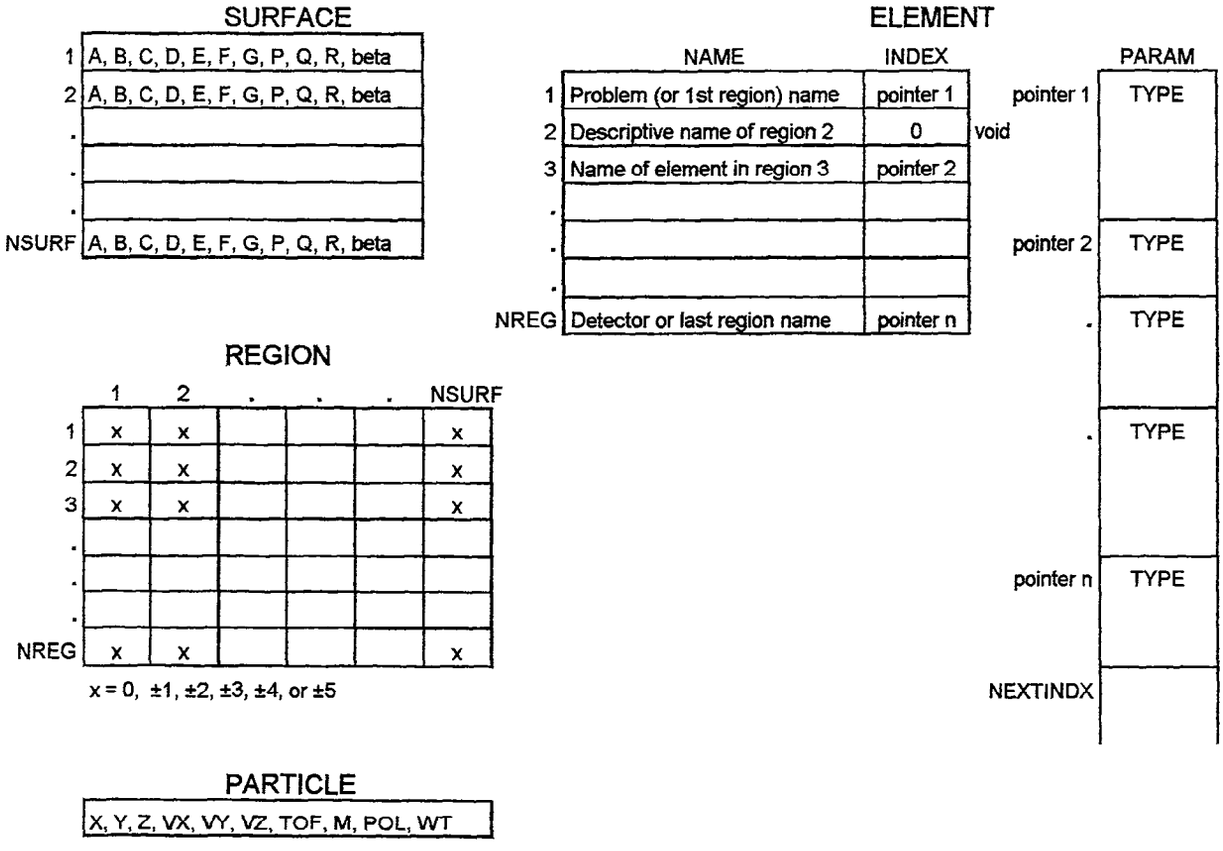

Figure 2. Structures used in MCLIB.

4. Program Structures

The relationships of the structures are shown schematically in fig. 2. The library source code is available in Fortran 77 with VAX structure extensions (F77/VAX), and also in Fortran 90 (F90). Unfortunately the F90 syntax did not adopt the relatively widespread F77/VAX standard, most distressingly by using "%" instead of "." as the member pointer in a structure!

In F77/VAX, each surface is a RECORD of type /SURFACE/, and elements are referenced as (*e.g.*) SURFACE.G. In F90, the surfaces are defined as derived TYPE (SURFACE), and element references are of the form SURFACE%G. Similarly, a geometric region is a RECORD of type /REGION/ or a derived TYPE (REGION); the structure in either case is a vector *IGEOM* of 2-byte integers, of length equal to the maximum allowed number of surfaces. An additional structure, MC_GEOM, contains the numbers of surfaces and regions in the problem, *NSURF* and *NREG*, and arrays of surface and region structures. Information about elements is contained in a structure called MC_ELEMENT which includes *NAME* and *INDEX* arrays, the parameter block *PARAM*, and the pointer *NEXTINDX* to the next available location in *PARAM*.

The final structure is PARTICLE, which includes the position, velocity, time of flight, mass (1 for a neutron), polarization (not yet implemented in the code), and statistical weight of a particle. A purely "analog" Monte Carlo traces each individual neutron until it is either lost or detected. MCLIB uses "weighted" neutrons, and in many of the processes the statistical weight is multiplied by the probability of survival instead of using a random number to decide whether to terminate the history ("Russian Roulette"). This is especially beneficial when scattering probability is small, as in subcritical reflection. To track more long-wavelength neutrons (which in general have larger scattering probability), the source distribution used is $\lambda^2 I(\lambda)$ instead of $I(\lambda)$ and the initial weight is proportional to $1/\lambda^2$. The tallied results are then the sum of detected neutron weights. The relative error in each bin, however, depends on the number of histories recorded.

The F77/VAX and F90 structure definitions follow. As compiled, the dimensions of the arrays are *MAXS* = 150, *MAXR* = 100, and *MAXP* = 800. For use in coding, all structure definitions are included in file MC_GEOM.INC (Appendix A).

F77 / VAX

```
STRUCTURE /SURFACE/
   REAL*4 A,B,C,D,E,F,G,P,Q,R
   REAL*4 BETA
END STRUCTURE

STRUCTURE /REGION/
   INTEGER*2 IGEOM(MAXS)
END STRUCTURE

STRUCTURE /MC_ELEMENT/
   CHARACTER NAME(MAXR)*40
   INTEGER*4 NEXTINDX, INDEX(MAXR)
   REAL*4    PARAM(MAXP)
END STRUCTURE

STRUCTURE /MC_GEOM/
   INTEGER*4 NSURF,NREG
   RECORD /SURFACE/ SURFACE(MAXS)
   RECORD /REGION/  REGION(MAXR)
END STRUCTURE

STRUCTURE /PARTICLE/
   REAL*4 X, Y, Z, VX, VY, VZ
   REAL*4 TOF, M, POL, WT
END STRUCTURE
```

F90

```
TYPE SURFACE
   SEQUENCE
   REAL 4:: A,B,C,D,E,F,G,P,Q,R
   REAL 4:: BETA
END TYPE SURFACE

TYPE REGION
   INTEGER 2:: IGEOM(MAXS)
END TYPE REGION

TYPE MC_ELEMENT
   CHARACTER   NAME(MAXR)*40
   INTEGER 4:: NEXTINDX, INDEX(MAXR)
   REAL 4::    PARAM(MAXP)
END STRUCTURE

TYPE MC_GEOM
   SEQUENCE
   INTEGER 4:: NSURF,NREG
   TYPE (SURFACE) SURFACE(MAXS)
   TYPE (REGION)  REGION(MAXR)
END TYPE MC_GEOM

TYPE PARTICLE
   SEQUENCE
   REAL 4:: X, Y, Z, VX, VY, VZ
   REAL 4:: TOF, M, POL, WT
END TYPE PARTICLE
```

5. Subroutine Library

Complete descriptions, calling sequences, revision history, and externals of all of the library subroutines are given in Appendix B. The following listing divides the subroutines into (somewhat arbitrary) categories, and includes the latest modification date and an abbreviated description. Note that if the operating system does not include the function RAN(ISEED), then the function must be provided as part of the library.

Vector analysis and transport

ANGLI	03 Feb 94	angle of incidence
DIST	23 Mar 95	distance to a surface
DTOEX	06 Mar 95	distance to nearest boundary
ELSCAT	26 Aug 95	do elastic scattering
LIGHTRFL	19 Mar 85	light reflection probability
LMONOCRM	21 Sep 95	reflection by crystal monochromator
LREFLCT	07 Jan 85	neutron reflection probability
MOSAIC	27 Jan 95	angle of incidence with mosaic spread
MOVEX	19 Apr 94	move a particle
NEXTRG	29 Jun 95	find region across boundary
N_SOURCE	29 Sep 95	get source neutron
GET_SPACE		get phase space of source
OPERATE	26 Aug 95	find what happens to particle within region
EXIT_REG		find what happens to particle leaving region
OPTICS	03 Feb 94	photon at region boundary
RFLN	03 Feb 94	do reflection
SNELL	03 Feb 94	apply Snell's law
TESTIN	29 Jun 95	find if within region
WHICHR	03 Feb 94	find what region particle is in
WOBBLE	03 Feb 94	angle of incidence at wavy surface

Material properties and scattering functions

ATTEN_Al	28 Jan 93	attenuation of Al
ATTEN_Be	25 Jan 95	attenuation of Be
ATTEN_X	14 Aug 95	attenuation of single-crystal filter
KERNEL	03 Apr 95	inelastic scattering kernel
PLQSPHR	06 Mar 95	probability from spherical scatterer
POWDER	14 Jul 95	scatter from polycrystalline powder
REFLAYER	07 Feb 95	reflection probability from multiple layers

Random distributions

IKDACARP	27 Sep 95	random sample from Ikeda-Carpenter
ORRAND	11 Mar 95	random unit vector
PLCNVL	11 Mar 95	probability from convolution of top-hats
PLEXP	16 Feb 95	probability from exponential
PLNORM	11 Mar 95	probability from normal
PLNRMTBL	13 Feb 95	probability from table vs. normal distribution
PLPOISSN	18 Mar 95	probability from Poisson
PLTIME	05 Sep 95	probability from parametrized emission time
PLTRNGL	04 Jan 85	probability from triangle
RAN	various	random number; platform dependent
RAN0	86	desequentialized random number
RNDCRCL	11 Mar 95	random point in unit circle

General utilities

DIGITS	05 Dec 87	convert number to string
GAMMLN	92	$\ln(\Gamma(x))$

GET_BINS	26 Jul 95	find detector/time bins
GET_RHO	16 Oct 95	find scattering-length density
GINI	05 Feb 92	standard deviation by Gini statistic
HUNT	13 Apr 87	find index in array
INTERP	84	interpolate in array
NORM	78	normalize unit vector
READ_1D	26 Jul 95	read 1-D block ASCII data file
READ_2D	21 Sep 95	read 2-D block ASCII data file
REALOUT	16 Aug 95	output array of REAL*4 numbers in block ASCII

Time-dependent devices

GRAV_FOC	07 Apr 94	gravity focuser
XCHOPPER	15 Mar 93	disk or blade chopper

Subroutine OPERATE and its other entry point EXIT_REG play special roles in the transport process. As can be inferred from the abstract in Appendix B, if this subroutine is called when a neutron enters a new region, then the routine will determine what happens. Possible results on exit from OPERATE include detection or loss of the neutron, exiting the region with reduced statistical weight (partial absorption), splitting the neutron into a transmitted and a scattered particle with the sum of statistical weights equal to the original weight, or a transform of the coordinate system of the problem. Coordinate transforms are applied for element types made up of sub-regions (*e.g.,* Soller slits and benders), elements which change the beam direction (benders and monochromaters), and time-dependent devices (gravity focuser). In order to assure that the coordinate system is properly restored when the neutron leaves the region, EXIT_REG must be called; this is flagged by using ±5 as the integer defining all exit surfaces from such a region.

6. Neutron Source Functions

Subroutines NSOURCE and PLTIME are called to generate source neutrons, using table lookup to select the velocity and a parametrized model to select the emission time. (If the length of the lookup table is 1, the velocity is a triangular or delta-function distribution; if the thermal decay constant is ≤ 0, emission time is 0.) The table and parameters are generally read from a file derived either from experimental measurements or from a detailed Monte Carlo simulation of a target/moderator/reflector system. The example given below uses a coupled liquid H_2 moderator with a 40-cm thick Be reflector on a spallation source, computed with MCNP [5], but the procedure would be the same for an experimental spectrum measurement. The energy spectrum from the MCNP output is shown in fig. 3. Program MKNRMTBL is provided to convert the spectrum. To improve sampling at long wavelengths, the data are multiplied by λ^2 before the cumulative sum is formed (the neutron is given an initial statistical weight proportional to $1/\lambda^2$ to account for this). The cumulative sum of the weighted table is compared to the integral of a Gaussian (*vs.* log E) fitted to the weighted data to form the table; that is, for equal steps in the argument of the Gaussian, its integral is evaluated and the cumulative sum is interpolated to find the corresponding neutron energy, which is then tabulated as $\log_{10}(E$ / 1 meV). To sample the neutron energy, a random deviate is chosen from a Gaussian distribution and that value is used to interpolate in the table ("transform" method [6]). This provides sharp detail over the peak of the spectrum and coarser interpolation in the wings, which may extend to more than 5 standard deviations.

The model for the time distribution is the sum of an epithermal and a thermal term convoluted with a Gaussian, added using a switch function [7,8] of the form $\exp[-(\lambda_0/\lambda)^P]$. This form was

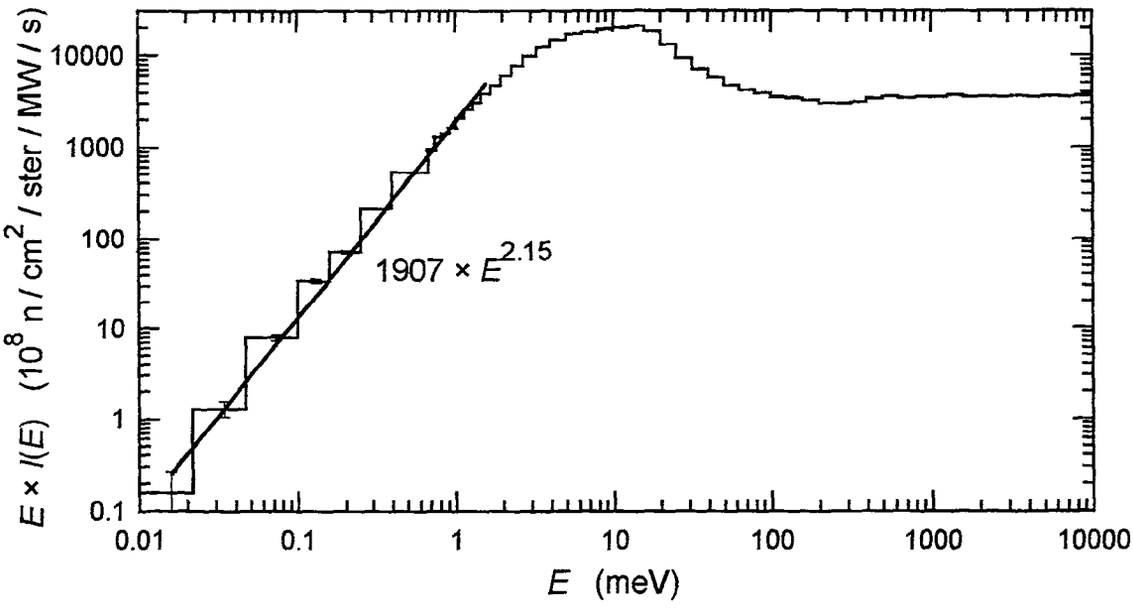

Figure 3. Neutron source energy distribution, as computed with the MCNP code.
Coupled liquid hydrogen moderator (equal fractions ortho and para), flux-trap geometry, 40-cm Be inner reflector, and Pb outer reflector (both reflectors are D_2O cooled). A power law was fitted to the low-energy regime to interpolate the histogram.

chosen because the convolution is easy in Monte Carlo; note however that a function to sample an Ikeda-Carpenter pulse shape distribution [7] has now been added to the library. Adequate fits can be made to most source terms using two exponentials; the epithermal (and the two parameters of the Gaussian) are proportional to wavelength, and the thermal time constant is independent of wavelength. Including the switch function, the total number of parameters in the model is then six. For the hybrid Be/Pb reflector case shown here, however, the fit with just two exponentials is not adequate and the thermal term itself must be a linear combination of two exponentials, for a total of eight parameters. Neutrons escaping from the moderator surface in the MCNP run [5] were tallied *vs.* time for 18 (logarithmic) wavelength bins from 0.09 to 15 Å; fig. 4 shows the data for one such bin, from 0.9 to 1.2 Å. Since the exponential decay after 1000 μs is constant for all wavelengths, the data from 0.9 to 15 Å were summed and a least-squares fit was made over the time range 1200–6000 μs, giving a thermal time constant $\tau_1 = 610$ μs. Since the early (epithermal) parameters are all proportional to λ, the early-time data can be summed after binning *vs.* (t/λ). (The variable t/λ is equivalent to the reduced time vt used in ref. [7].) A least-squares fit in the t/λ range 1–30 μs/Å gave the values epithermal exponential $\eta = 8.67$ μs/Å, delay $\Delta = 5.68$ μs/Å, and width $\sigma = 2.08$ μs/Å. Given these fits to the early and late times, the additional exponential term was estimated ($\tau_2 = 170$ μs, ratio $R = 2/3$). Then the ratios of thermal to epithermal terms were extracted, and the two parameters of the switch function determined ($\lambda_0 = 0.86$ Å, $P = 2.63$). The line in fig. 4 is an example of the resulting fit, evaluated at $\lambda = 1.0$ Å where all three components are significant.

7. Sample Program Output

Sample program source codes `LQDGEOM.FOR` and `MC_RUN.FOR` will be distributed with all copies of the library, but because of their lengths are not included in this report. Communication between the two programs is through a geometry file, such as the following example, `LPSS.GEO`. The first part of the file is not used by the succeeding program, but contains text to identify the problem and to give the parameters entered by the user.

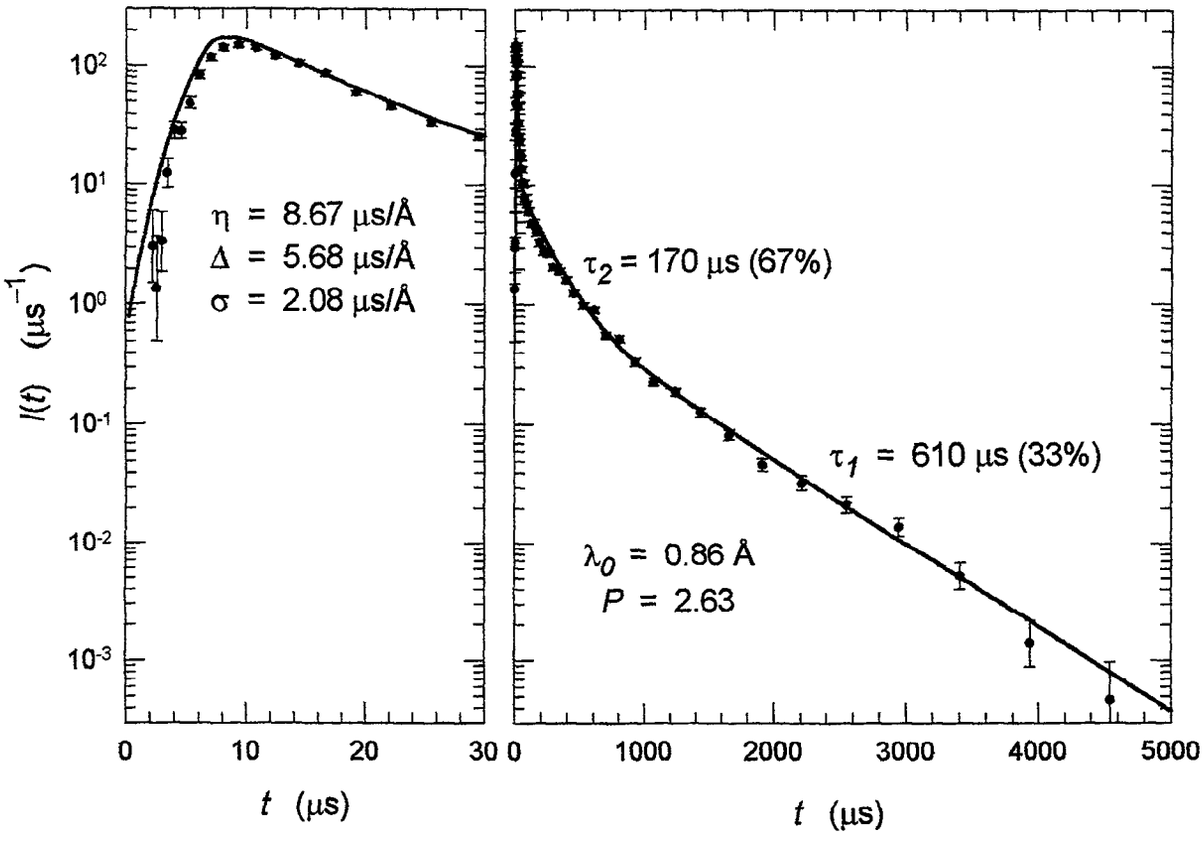

Figure 4. Source time distribution at 1.0 Å.

Points are the MCNP "data," and the line is the model fit. At this wavelength, near the midpoint of the switch function, the early "epithermal" and the two late "thermal" exponential terms are all seen.

```
Geometry code version: F90, June 30, 1995, P.A.Seeger
LQD Geometry file: lpss.geo
Proton pulse rate = 60.0 Hz, width = 1000.0 us, max wavelength 15.1 A
Sample at  7.00 m, Detector at 13.00 m from moderator
Sample diameter = 10.00 mm
Spectrum and lineshape file: \mclib\Pb40Be13.tbl
   T0 Chop at  2.60m, open  0.827ms, close  14.839ms, rms  40.0us, v 56.55m/s
O'lap Chop at  3.10m, open  7.257ms, close  12.281ms, rms  20.0us, v 94.25m/s
Frame Chop at  6.00m, open 16.253ms, close  22.874ms, rms  20.0us, v 94.25m/s
Collimation:  entrance aperture radius  7.53 mm at position  2.500 m
              exit                      4.44 mm              6.800 m
Moderator half-width and half-height = 0.050 m
          spot radius  9.32 mm, penumbra radius 14.48 mm
Time range  34370.0 -  49665.1 us
Sample Transmission at Lmax (15.11 A) is 0.600
Total thickness of Al = 12.0 mm
Detector half-width 0.320 m,  pixel 5.00 mm,  rms 3.40 mm
         penumbra radius 21.70 mm,  min angle 4.78 mr
Q-range:  0.00200 - 0.03134 /A
Gravitational droop  2.21 -   4.62 mm
```

The next three lines give the numbers of surfaces and regions and the length of the parameter block. They are required, and the remainder of the file must follow in order:

```
SURFACES      25
REGIONS       28
PARAMETERS   189
```

Each surface definition is given on one line; zero entries may be left null:

`,,,,,1/`	PZ (plane perpendicular to z-axis) at z = 0
`1,,1,,,,-.0036/`	CZ (cylinder on z-axis), radius 60 mm
`,,,,,1,-2.498/`	PZ at z = 2.498 m
`486749,,486749,,-1,15.5,-60.0625/`	Cone on z-axis
`,,,,,1,-2.5/`	PZ at z = 2.5 m
`,,,,,1,-2.6/`	PZ at z = 2.6 m
`1,,1,0.6,,,-.2025/`	Cylinder parallel to z-axis, offset y = –0.3 m, radius 0.335 m
`,,,,,1,-2.9/`	PZ at z = 2.9 m
`1,,1,,,,-.0036/`	CZ, radius 60 mm
`,,,,,1,-3.1/`	PZ at z = 3.1 m
`1,,1,0.6,,,-.2025/`	Cylinder parallel to z-axis, offset y = –0.3 m, radius 0.335 m
`,,,,,1,-3.102/`	PZ at z = 3.102 m
`,,,,,1,-6/`	PZ at z = 6.0 m
`1,,1,0.6,,,-.2025/`	Cylinder parallel to z-axis, offset y = –0.3 m, radius 0.335 m
`,,,,,1,-6.002/`	PZ at z = 6.002 m
`,,,,,1,-6.8/`	PZ at z = 6.8 m
`585518,,585518,,-1,6.8,-11.56/`	Cone on z-axis
`,,,,,1,-6.802/`	PZ at z = 6.802 m
`,,,,,1,-7/`	PZ at z = 7.0 m
`,,,,,1,-7.001/`	PZ at z = 7.001 m
`,,,,,1,-7.013/`	PZ at z = 7.013 m
`1,,1,,,,-0.25/`	CZ, radius 0.5 m
`,,,,,1,-13/`	PZ at z = 13.0 m
`,,,,,1,-12.95/`	PZ at z = 12.95 m
`1,,1,,,,-5.6169E-4/`	CZ, radius 23.7 mm

Each region is a line with an entry for each surface:

```
-1  0  0  0  0  0  0  0  0  0  0  0  0  0  0  0  0  0  0  0  0  0  0  0  0
-1  0  0  0  0  0  0  0  0  0  0  0  0  0  0  0  0  0  0  0  0  0  0  0  0
 1 -4 -1  0  0  0  0  0  0  0  0  0  0  0  0  0  0  0  0  0  0  0  0  0  0
 1  4 -4  0  0  0  0  0  0  0  0  0  0  0  0  0  0  0  0  0  0  0  0  0  0
 0  0  1 -4 -1  0  0  0  0  0  0  0  0  0  0  0  0  0  0  0  0  0  0  0  0
 0  0  1  4 -4  0  0  0  0  0  0  0  0  0  0  0  0  0  0  0  0  0  0  0  0
 0  0  0  0  1 -1  0  0  0  0  0  0  0  0  0  0  0  0  0  0  0  0  0  0  0
 0  0  0  0  0  1 -4 -1  0  0  0  0  0  0  0  0  0  0  0  0  0  0  0  0  0
 0  0  0  0  0  1  4 -4  0  0  0  0  0  0  0  0  0  0  0  0  0  0  0  0  0
 0  0  0  0  0  0  0  1 -4 -1  0  0  0  0  0  0  0  0  0  0  0  0  0  0  0
 0  0  0  0  0  0  0  1  4 -4  0  0  0  0  0  0  0  0  0  0  0  0  0  0  0
 0  0  0  0  0  0  0  0  0  1 -4 -1  0  0  0  0  0  0  0  0  0  0  0  0  0
 0  0  0  0  0  0  0  0  0  1  4 -4  0  0  0  0  0  0  0  0  0  0  0  0  0
 0  0  0  0  0  0  0  0 -4  0  0  1 -1  0  0  0  0  0  0  0  0  0  0  0  0
 0  0  0  0  0  0  0  0  4  0  0  1 -4  0  0  0  0  0  0  0  0  0  0  0  0
 0  0  0  0  0  0  0  0  0  0  0  0  1 -4 -1  0  0  0  0  0  0  0  0  0  0
 0  0  0  0  0  0  0  0  0  0  0  0  1  4 -4  0  0  0  0  0  0  0  0  0  0
 0  0  0  0  0  0  0  0 -4  0  0  0  0  0  1 -1  0  0  0  0  0  0  0  0  0
 0  0  0  0  0  0  0  0  4  0  0  0  0  0  1 -4  0  0  0  0  0  0  0  0  0
 0  0  0  0  0  0  0  0  0  0  0  0  0  0  0  1 -4 -1  0  0  0  0  0  0  0
 0  0  0  0  0  0  0  0  0  0  0  0  0  0  0  1  4 -1  0  0  0  0  0  0  0
 0  0  0  0  0  0  0  0  0  0  0  0  0  0  0  0  1 -1  0  0  0  0  0  0  0
 0  0  0  0  0  0  0  0  0  0  0  0  0  0  0  0  0  1 -1  0  0  0  0  0  0
 0  0  0  0  0  0  0  0  0  0  0  0  0  0  0  0  0  0  1 -1  0  0  0  0  0
 0  0  0  0  0  0  0  0  0  0  0  0  0  0  0  0  0  0  0  1 -4 -1 -11 14
 0  0  0  0  0  0  0  0  0  0  0  0  0  0  0  0  0  0  0  1  4 -4  0  0
 0  0  0  0  0  0  0  0  0  0  0  0  0  0  0  0  0  0  0  0  1  0  0
 0  0  0  0  0  0  0  0  0  0  0  0  0  0  0  0  0  0  0  0 -1  1 -4
```

The *NAME* associated with each region; the first *NAME* is the problem title, and the second is the title of the source file:

```
 7m, 13m, 15A, 60Hz (1000us), Q=0.01/A
H2 (50/50,64/16), Fluxtrap, 40-cm Be, Pb
Shutter penetration
Bulk shield
Circular entrance aperture
Collimator entrance
Drift to T0 chopper
T0 Chopper
T0 chopper shielding
Collimator pipe
Collimator shielding
Frame-overlap chopper
Overlap chopper shielding
Collimator pipe
Collimator shielding
Frame-definition chopper
Frame-definition chopper shield
Collimator pipe
Collimator shielding
Circular exit aperture
Collimator exit
Drift to Sample
Sample
Aluminum
Secondary Flight Path
Secondary flight Path shielding
Detector
Beamstop
```

Next is the list of *INDEX* pointers into the parameter block:

```
   1   18    0  133    0  134    0  135  142    0  143  144  151    0  152
 153  160    0  161    0  162    0  163  166  167  168  169  189
```

Finally, the parameter block, including the source wavelength distribution:

```
90,-0.05,0.05,-0.05,0.05,2.5,.007525,6.8,.00444333,,8.95436-5,.0818145,16666.67,-1000,18,,,
91,102,47.6,11.24,5.83333E16,610,170,.667,8.67,5.68,2.08,.86,2.63,
  -1.700001,-1.698674,-1.69677,-1.694059,-1.69023,-1.684864,-1.677405,-1.667116,-1.653036,
  -1.633922,-1.608176,-1.579874,-1.544875,-1.49911,-1.453015,-1.394889,-1.336073,-1.27017,
  -1.198053,-1.128077,-1.054727,-.978697,-.90117,-.828609,-.75508,-.680891,-.608064,
  -.540398,-.472038,-.403717,-.342582,-.2799292,-.2202448,-.1641208,-.1068591,-.0565061,
  -.00302955,.0482707,.0975991,.1475286,.1969256,.2461485,.2951157,.341733,.387269,.432616,
  .475812,.519135,.56161,.603647,.645207,.685663,.727038,.767961,.808221,.852178,.893306,
  .937217,.978778,1.020489,1.062588,1.100546,1.141591,1.177922,1.213727,1.252556,1.286119,
  1.326629,1.370402,1.412875,1.467081,1.520122,1.581781,1.650554,1.722381,1.800968,
  1.889334,1.981707,2.078442,2.177055,2.278023,2.383607,2.487587,2.585048,2.668664,
  2.739018,2.795598,2.847828,2.88669,2.918281,2.943239,2.960935,2.973372,2.982054,2.988064,
  2.992237,2.995075,2.996995,2.998247,2.999082,2.999666,3,,,
20,9.42478E-5,117.0279,7257.36,12280.94,20,16666.67,,,
20,9.42478E-5,82.747,16253.48,22874.19,20,16666.67,,,,
30,.0337991,0.01,2,50,,
43,23,1.89712,34370,49665.1,37,0.01,0.1,,16666.67,-0.32,0.32,128,0.005,.0034,
   -.3231944,.3168057,128,0.005,.0034,23/
```

The program MC_RUN asks the user for the geometry file name, the number of histories to be detected, and a starting value for the random-number generator. The user chooses whether the recorded monitor spectrum is to represent a sample-in or a sample-out measurement. Options

are also given to convert the final output histograms, which are sums of weights, to integers. There are two ways to do this. If one wishes the error bars on the output to be similar to a Poisson distribution so they look like real data, and if the error from the number of histories is small, then the value for each bin can be replaced by a sample from a Poisson distribution with mean equal to the tally for that bin. If the error bars are already appropriate, then a simple Russian roulette procedure is to add a random number (on the range 0 – 1) and truncate the result to an integer. The following file is the output using the above geometry file. The running time to detect 300000 neutron histories (5.4×10^6 starts) was 4.55 hours on a 486/66 PC; the estimated experiment time is 10.5 seconds (at 1 MW proton beam power).

```
MONTE CARLO SIMULATION OF A NEUTRON SCATTERING INSTRUMENT
 MC_RUN code version: PC, September 17, 1995, P.A.Seeger
```

(At this point the text from the front of the geometry file is reproduced)

```
 Successfully read input file with  25 surfaces,  28 regions,
                                and 189 element parameters.
```

A test particle is sent along the instrument axis as a simple sanity check:

```
 Beam elements along the instrument axis:
 Surf  1, Z =   .000 m, enter reg  3, Shutter penetration
 Surf  3, Z =  2.498 m, enter reg  5, Circular entrance aperture
 Surf  5, Z =  2.500 m, enter reg  7, Drift to T0 chopper
 Surf  6, Z =  2.600 m, enter reg  8, T0 Chopper
 Surf  8, Z =  2.900 m, enter reg 10, Collimator pipe
 Surf 10, Z =  3.100 m, enter reg 12, Frame-overlap chopper
 Surf 12, Z =  3.102 m, enter reg 14, Collimator pipe
 Surf 13, Z =  6.000 m, enter reg 16, Frame-definition chopper
 Surf 15, Z =  6.002 m, enter reg 18, Collimator pipe
 Surf 16, Z =  6.800 m, enter reg 20, Circular exit aperture
 Surf 18, Z =  6.802 m, enter reg 22, Drift to Sample
 Surf 19, Z =  7.000 m, enter reg 23, Sample
 Surf 20, Z =  7.001 m, enter reg 24, Aluminum
 Surf 21, Z =  7.013 m, enter reg 25, Secondary Flight Path
 Surf 24, Z = 12.950 m, enter reg 28, Beamstop
 Surf 23, Z = 13.000 m, enter reg 27, Detector
 ** No exit found from Detector
```

Having found the source, the sample, and the detector, it is safe to proceed:

```
 Number of detector bins = 128 x 128 ( 90 radial), and   37 spectrum slices
 Output data forms: T       RT
 Initial random number = 075BCD15,  300000 neutrons to be detected
 Moderator phase space to be sampled =   .00060 mm**2-ster
                                      x 6.82 e-fold of energy
 Source brightness = 5.833E+16 n/ster/m**2/MW/s
```

A tally is kept of how much neutron statistical weight was absorbed in each element:

```
t     7m, 13m, 15A, 60Hz (1000us), Q=0.01/A   MC__951002_112859
Summary of neutron losses by region:
   11.77% lost in region  3, Shutter penetration
     .02% lost in region  6, Collimator entrance
   13.30% lost in region  8, T0 Chopper
   73.62% lost in region 12, Frame-overlap chopper
     .80% lost in region 16, Frame-definition chopper
     .00% lost in region 20, Circular exit aperture
     .00% lost in region 23, Sample
     .06% lost in region 24, Aluminum
     .00% lost in region 25, Secondary Flight Path
```

```
     .00% lost in region 27, Detector
     .00% lost in region 28, Beamstop

Beam is centered at (   -.02,  -3.19) mm, with rms (  7.7,   7.7) mm
 Total histories tracked:  5421391 (3.665E+08 neutrons)
 Detected in Transmission:  303763 (9.975E+05,    .27%)
 Detected in Scatter Mode:  300000 (5.191E+05,    .14%)
 Beam power on target:       10.5     Mw-s
 Bad-Frame neutrons passed:          0.000E+00
 Bad-Frame neutrons detected:        0.000E+00
 Final random number: 0FB3ECE2
```

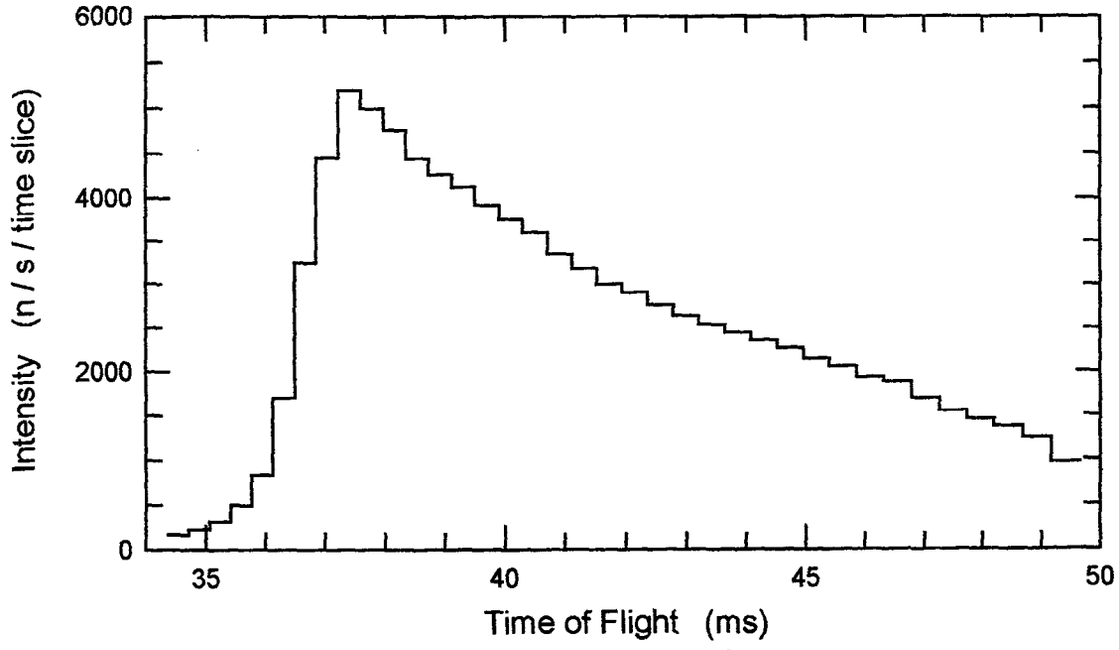

Figure 5. Time-of-flight spectrum of transmitted neutrons for LPSS test case.
At 13 m flight path length, the corresponding wavelength range is 10.5–15.1 Å. The source is a 1-MW spallation source with a coupled liquid H_2 moderator, pulsed at 60 Hz.

The output data files include header information and blocks of ASCII data for bin boundaries, data, and standard deviations. The values in the blocks are "," separated and "/" terminated as in the geometry file shown above. Data include the transmitted spectrum histogram (fig. 5) and a 2-dimensional histogram of counts integrated in radial zones on the detector for each time slice (fig. 6). By converting the radial data to Q for each individual wavelength (time slice) before combining, the time-of-flight wavelength resolution is maintained. The final result for this test case is shown in fig. 7.

8. Future Directions

It is the intention of the author that MCLIB remain in the public domain (see copyright notice in Appendix B). The most recent versions of the library and auxiliary codes as described above will continue to be available to any interested users from the author or from the Los Alamos Neutron Science Center (LANSCE) *via* Internet file transfer. Input of ideas, algorithms, and/or (public) code modules to expand the library is requested and encouraged, and will be acknowledged. Element types 70 through 79 are reserved for individual non-standard use; please contact the author for assignment of permanent type numbers.

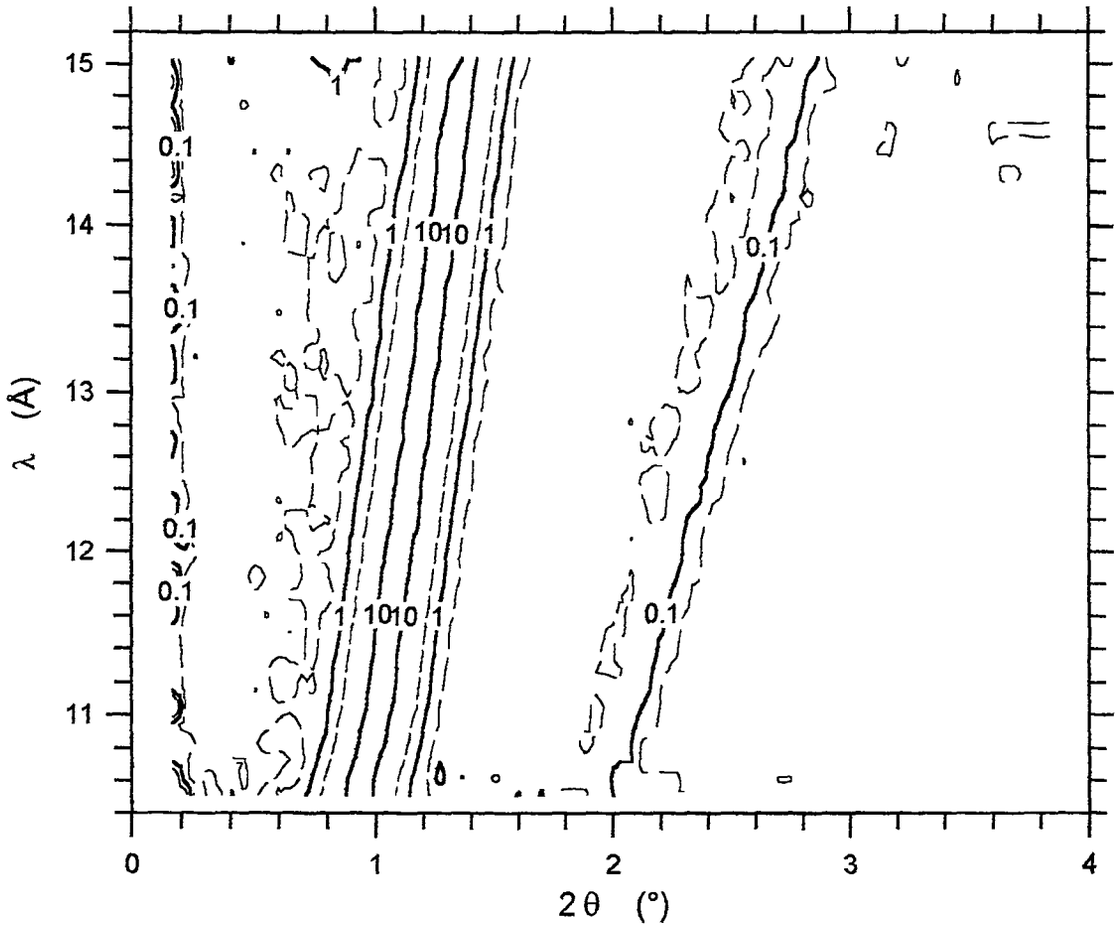

Figure 6. Relative count rate in detector *vs.* radial position and time of flight, for test case.
Time of flight has been converted to wavelength and detector radial zone to scattering angle (2θ). Contour intervals are logarithmic.

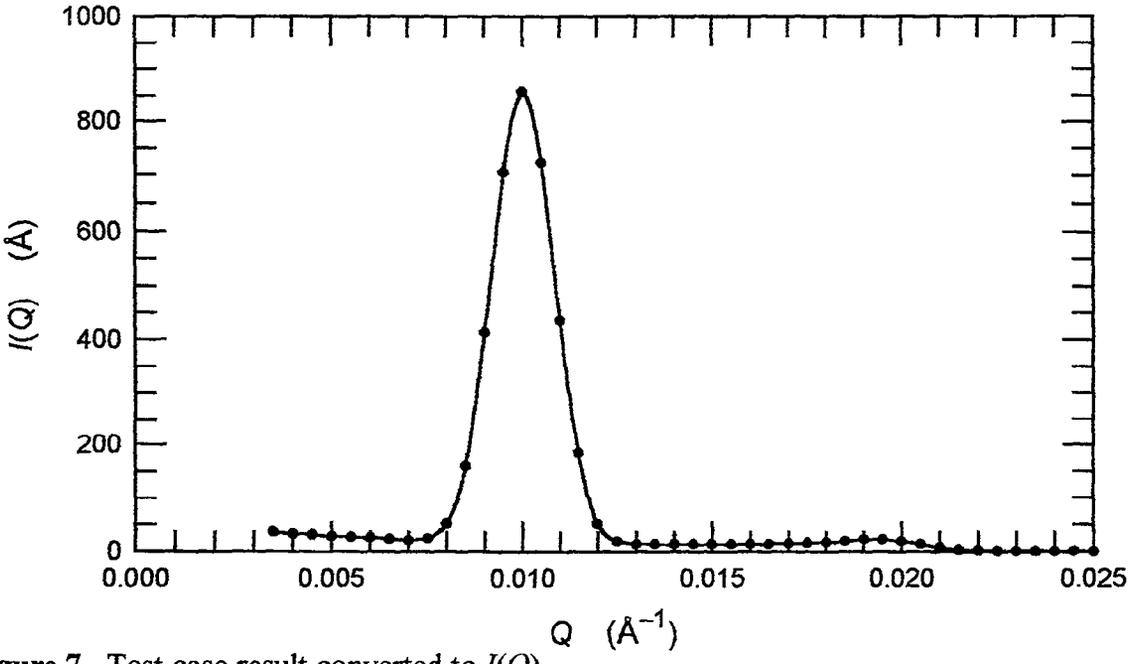

Figure 7. Test case result converted to $I(Q)$.
The scattering "sample" was a δ–function in Q at $Q = 0.010$ Å^{-1}. The standard deviation of the result is thus the resolution of the instrument at this value of Q; in this case $\sigma = 0.0009$ Å^{-1}.

A parallel (but separate) effort at LANSCE is developing a user interface (based on the Smalltalk language) which will greatly simplify design of new instrument configurations by facilitating creation of the geometry file [9]. The MCLIB library will be modified as necessary to support this project, and to include new features, such as polarization.

9. Acknowledgments

This effort has been supported historically by the U. S. Department of Energy under contract W-7405-ENG-36, and the author is grateful to the Los Alamos Neutron Science Center for their continued interest and support. Many (hopefully *most*) of the individuals who have contributed directly are listed in the text. I am also grateful to Jack Carpenter and Kent Crawford (IPNS) for making comments and suggestions for this manuscript.

10. References

[1] M. W. Johnson and C. Stephanou, "MCLIB: A Library of Monte Carlo Subroutines for Neutron Scattering Problems," Rutherford Laboratory report RL-78-090, September, 1978; M. W. Johnson, "MCGUIDE: A Thermal Neutron Guide Simulation Program," Rutherford and Appleton Laboratories report RL-80-065, December, 1980.

[2] P. A. Seeger and R. Pynn, "Resolution of Pulsed-Source Small-Angle Neutron Scattering," *Nucl. Inst. Methods* **A245** (1985) 115–124.

[3] P. A. Seeger, "Monte Carlo Calculations for the Optimisation of the Beam Optics of the LOQ Spectrometer," report to Rutherford Appleton Laboratory, 28 April, 1994.

[4] P. A. Seeger, G. S. Smith, M. Fitzsimmons, G. A. Olah, L. L. Daemen, and R. P. Hjelm, Jr., various contributions, Instrumentation for a Long-Pulse Spallation Source Workshop, Lawrence Berkeley Laboratory, Berkeley, CA, April 18–21, 1995.

[5] E. J. Pitcher, G. J. Russell, P. A. Seeger, and P. D. Fergusson, "Performance of long-pulse source reference target-moderator-reflector configurations," Proceedings of the 13th Meeting of the International Collaboration on Advanced Neutron Sources, October 11–14, 1995, Paul Scherrer Institut, Villigen, Switzerland.

[6] W. H. Press, S. A. Teukolsky, W. T. Vettering, and B. P. Flannery, *Numerical Recipes,* 2nd Edition (Cambridge University Press, 1992), section 7.3.

[7] S. Ikeda and J. M. Carpenter, "Wide-energy-range, high-resolution measurements of neutron pulse shapes of polyethylene moderators," *Nucl. Inst. Methods* **A239** (1985) 536–544.

[8] R. A. Robinson and J. M. Carpenter, "On the use of switch functions in describing pulsed neutron moderators," *Nucl. Inst. Methods* **A307** (1991) 359–365.

[9] T. G. Thelliez, L. L. Daemen, P. A. Seeger, and R. P. Hjelm, Jr., "A user-friendly geometry interface for the Monte Carlo neutron optics code MCLIB," Proceedings of the 13th Meeting of the International Collaboration on Advanced Neutron Sources, October 11–14, 1995, Paul Scherrer Institut, Villigen, Switzerland.

Appendix A
Files MC_GEOM.INC, MC_ELMNT.INC and CONSTANT.INC

Appendix B
Subroutine Abstracts

Editors' note:
In view of the length of these appendices, the author has agreed to our request to omit them from the published proceedings. The author has assured us that he will be pleased to provide a copy to anyone who is interested (see e-mail address on the title page). In particular, the file MCLIB.TXT containing a copy of the text of this article including the appendices may be obtained by anonymous ftp from

```
azoth.lansce.lanl.gov/pub/mclib.txt
```

The copyright notice referenced as being in Appendix B follows.

See also late submission paper I-26